Study on improving the modulatory effect of rhythmic oscillations by transcranial magneto-acoustic stimulation

Ruxin Tan[1], Ren Ma[1], Fangxuan Chu[1], Xiaoqing Zhou[1], Xin Wang[1], Tao Yin[1], Zhipeng Liu[1]

***Abstract*—In hippocampus, synaptic plasticity and rhythmic oscillations reflect the cytological basis and the intermediate level of cognition, respectively. Transcranial ultrasound stimulation (TUS) has demonstrated the ability to elicit changes in neural response. However, the modulatory effect of TUS on synaptic plasticity and rhythmic oscillations was insufficient in the present studies, which may be attributed to the fact that TUS acts mainly through mechanical forces. To enhance the modulatory effect on synaptic plasticity and rhythmic oscillations, transcranial magneto-acoustic stimulation (TMAS) which induced a coupled electric field together with TUS's ultrasound field was applied. The modulatory effect of TMAS and TUS with a pulse repetition frequency of 100 Hz were compared. TMAS/TUS were performed on C57 mice for 7 days at two different ultrasound intensities (3 W/cm^2 and 5 W/cm^2). Behavioral tests, long-term potential (LTP) and local field potentials in vivo were performed to evaluate TUS/TMAS modulatory effect on cognition, synaptic plasticity and rhythmic oscillations. Protein expression based on western blotting were used to investigate the underlying mechanisms of these beneficial effects. At 5 W/cm^2, TMAS-induced LTP were 113.4% compared to the sham group and 110.5% compared to TUS. Moreover, the relative power of high gamma oscillations (50-100Hz) in the TMAS group (1.060±0.155%) was markedly higher than that in the TUS group (0.560±0.114%) and sham group (0.570±0.088%). TMAS significantly enhanced the synchronization of theta and gamma oscillations as well as theta-gamma cross-frequency coupling. Whereas, TUS did not show relative enhancements. TMAS provides enhanced effect for modulating the synaptic plasticity and rhythmic oscillations in hippocampus.**

***Index Terms*— transcranial ultrasonic stimulation (TUS); transcranial magneto-acoustic stimulation (TMAS); synaptic plasticity; rhythmic oscillations; hippocampus**

I. Introduction

SIGNIFICANT advances in neuroscience have identified the hippocampus as the core region for cognition [1, 2]. In cognition, Synaptic plasticity was the cytological basis [3]. The rhythmic oscillations reflect the intermediate level between neuron functions and cognitive behavior [4]. The hippocampus resides in a deep brain region and its size is small, with 1 mm in diameter and slightly less than 5 mm in length for mice [5]. Because of this, precise modulation is remained remarkably challenging. Transcranial ultrasound stimulation (TUS) with 0.25-1 MHz center frequency could penetrate the skull and intracranial tissues, with significant advantages in stimulation depth and spatial resolution up to millimeter-scale [6]. These features make TUS be of interest to modulate the hippocampus and improve cognition. At present, studies have shown the modulation of TUS on neurons, with TUS irradiation on hippocampal slices inducing the pyramidal neuronal activity [7, 8]. Studies have found that long-term in vivo TUS in the hippocampus induced sustained synaptic plasticity with an increased density of dendritic spines in normal rats [9]. Lasting TUS restored the strength phase amplitude coupling (PAC) between theta and gamma in AD model mice [10]. These studies indicate that TUS has modulatory effects on neurons, synaptic plasticity and rhythmic oscillations.

However, the modulation of TUS still has limitations in the present studies. Niu [11] found that lasting TUS has shown but a modest effect in raising presynaptic potentials, evoking only long-term depression, but not long-term potentiation. Huang [9] demonstrated that TUS increased excitatory spontaneous postsynaptic currents (EPSC) frequency in CA1 hippocampal pyramidal neurons, but showed no modulatory effect on EPSC amplitude, half-width, rise time and decay time. Xie [12] and Yuan's [13] studies showed that TUS enhanced the power and PAC strength of rhythmic oscillations only when the ultrasonic intensity reached 0.6MPa or exceeded 9.6W/cm^2. The studies above showed that the modulatory effects of TUS may not be efficient enough. It has been shown that the main mechanism of TUS neuromodulation is thought to excites neurons mechanically leading to the opening of specific mechanosensitive calcium channels [14, 15]. This may account for the inefficient modulatory effects of TUS.

This study was supported by the National Natural Science Foundation of China (81927806, 52077223, 52107241) and the CAMS Initiative for Innovative Medicine (No. 2021-I2M-1-058, 2022-I2M-2-003). Ruxin Tan, Ren Ma contributed equally to this work.

R. T. Author is with Chinese Academy of Medical Sciences & Peking Union Medical College, Institute of Biomedical Engineering, Tianjin 300192, China. (e-mail: tanruxin78@hotmail.com).

L. Z. Author is with Chinese Academy of Medical Sciences & Peking Union Medical College, Institute of Biomedical Engineering, Tianjin 300192, China. (e-mail: lzpeng67@163.com).

Supplementary material contains detailed METHODS.

Transcranial magneto-acoustic stimulation (TMAS) is an emerging noninvasive multi-physic deep stimulation, which combines ultrasonic excitation with a static magnet and forms a composite stimulation of coupled electric field and ultrasonic field (Fig. 1(a)) [16]. Li confirmed the existence of coupled electric fields and verified the feasibility of TMAS [17]. Yuan et al. [18]and Zhang et al. [19] investigated the mechanism of TMAS based on a computational model that TMAS altered neuron firing patterns. Wang Y. et al. showed that TMAS improved long-term potentiation and dendritic spine densities in the dentate gyrus in PD model mice [20]. Given its compound nature, Wang H. et al. [21] found that TMAS induced stronger electromyogram than TUS in the motor cortex of normal mice. Do combined mechanical and electrical stimulation serve to enhance the modulatory effects of hippocampal rhythmic oscillations and synaptic plasticity?

The aim of this study was to explore the effects of combined electrical and mechanical stimulation on synaptic plasticity and rhythmic oscillations. We compared the modulation effect of TMAS with that of TUS at 2 different ultrasound intensities to show the enhancement of TUS modulation with the addition of a coupled electric field. The multi-physic stimulation (TMAS) combined ultrasonic field and the coupled electric field would provide novel ways to improve the effectiveness of TUS.

II. METHODS

A. Animals

Eighty 2-month-old male C57NL/6J mice were purchased from HFK Bioscience Co., Ltd. (Beijing, China), and were randomly divided into 5 groups with equal number: the sham group, TUS_I group, TUS_II group, TMAS_I group, and TMAS_II group. The mice were housed under standard laboratory conditions (room temperature 24±2°C, 12 h light/dark cycle with lights on at 7:00 a.m., and water and food ad libitum). All experiments were approved by the Ethics Committee of the Institute of Biomedical Engineering.

B. Stimulation System and Parameters

As shown in Fig. 1(b), the TUS stimulation system was conducted by a focused ultrasound transducer (FP-1M, IOA-AC, China) with 1 MHz center frequency, a signal generator (AFG3252, Tektronix, USA), a power amplifier (HSA4101, NF, Japan), a vaporized anesthesia machine (0.5% isoflurane) and a stereotactic apparatus (SR-6R-HT, Narishige, Japan). For the TMAS stimulation system, a 0.3 T neodymium magnet was additionally used to generate the coupled electric field. Ultrasound parameters for rodent hippocampus referred to prior studies [9][22]. Intensity was set at 3 W/cm^2 for TUS_I and TMAS_I, and 5 W/cm^2 for TUS_II and TMAS_II, with a 100 Hz pulse repetition frequency and 5% duty cycle. Each mouse received 5 minutes of sonication. See Fig. 1(c) and Fig. 1(d) for pulse train and stimulation target.

C. Experiment procedure

The stimulation period consisted of 7 days. Twenty-four hours after the last stimulation, 8 mice in each group were subjected to in vivo local field potential (LFP) recording, long-term potentiation (LTP) induction from the perforant pathway (PP) to the dentate gyrus (DG) and western blot assay, and the other 8 mice were subjected to the open field test (OFT), the novel object recognition test (NOR) and the Morris water maze test (MWM), as shown in Fig.1(e). See the supplementary materials for the detail procedures.

D. LFP Analysis

1) **Power Spectral Density (PSD) Analysis**

A multiwindow spectral estimation method was used to calculate the power spectral density with a data window length of 10 s and 50% overlap. The 0.5-100 Hz band was extracted as the total power, and the relative power in theta band (3-8 Hz), low gamma band (30-50 Hz) and high gamma band (50-100 Hz) was normalized to the percentages across the total power.

2) **Phase-Phase Coupling**

The phase-locked values were used to measure the phase synchronization between the two brain regions. The phase-locked value [23] was then calculated according to (1).

$$PLV = \left| \frac{1}{N} \sum_{j=1}^{N} \exp\left(i\left[\varphi_x(t_j) - \varphi_y(t_j)\right]\right) \right| \quad (1)$$

The n:m phase-phase coupling [24] was used to evaluate the synchronization between different rhythms, where the ratio n:m represents n cycles of high-frequency oscillations stabilized for every m cycles of low-frequency oscillations. The radial distance, r, is derived from (2).

$$r_{n:m} = \left| \frac{1}{N} \sum_{j=1}^{N} \exp\left(i\left[m\varphi_{low}(j) - n\varphi_{high}(j)\right]\right) \right| \quad (2)$$

3) **Coherence**

Coherence [25] measures the linear correlation between two regions in frequency domain and was calculated from (3);

$$Coh_{xy}(f) = \frac{\left|S_{xy}(f)\right|^2}{S_{xx}(f)S_{yy}(f)} \quad (3)$$

4) **Phase-Amplitude Coupling**

The modulation index (MI) is used to quantify the strength of the phase-amplitude coupling between theta rhythms and low gamma or high gamma rhythms. See the supplementary materials for the details.

E. Western Blot

The procedure of western blot was described as previously published [26]. In this study, following primary antibodies were used: anti-SYP (1:20000; Abcam, ab32127), anti-PSD-95 (1:1000; Abcam, ab238135), anti-NR-2B (1:1000; Abcam, ab65783), anti-NR-2A (1:1000; CST, 4205), and anti-GABAAR (1:1000; Abcam, ab33299).

F. Statistical Analysis

The data are expressed as the mean ± standard error of the mean (SEM). First, independent samples t tests were used to compare the stimulation groups with the sham group to assess their facilitative or inhibitory modulatory effects. Then, two-way stimulation × intensity factorial analysis of variance (ANOVA) was used to assess the effects of stimulation and

intensity, followed by post hoc Bonferroni tests. All statistical analyses were performed by SPSS Software (version 21.0), and the significance level was set at 0.05.

III. RESULTS

A. TMAS and TUS both enhanced the short-term memory

The OFT was used to evaluate whether the stimulation process contributed to anxiety in mice. As shown in Fig. 2(a), there was no significant difference in exploration time in the central area between the stimulation group and the sham group, indicating that stimulation did not cause anxiety in mice.

The NOR (Fig. 2(b)) was performed to test short-term and long-term memory in mice. During the training session, the contact duration of the two objects was comparable among groups, as shown in Fig. 2(c). In the short-term testing session, the recognition index in the TUS_II, TMAS_I and TMAS_II groups was significantly higher than that in the sham group (TUS_II vs. sham: P=0.027; TMAS_I vs. sham: P=0.030; TMAS_II vs. sham: P=0.032), indicating that short-term memory was enhanced, as shown in Fig. 2(d). In the long-term testing session, the recognition index in the TUS_II, TMAS_I and TMAS_II groups was higher than that in the sham group, indicating a tendency to enhance long-term memory, while the differences were not significant. Stimulation × intensity ANOVA showed no main effects and no interaction effects in both the short-term memory and long-term memory.

B. TMAS improved spatial learning and memory

The initial MWM procedure (Fig. 3(a)) was used to assess the acquisition of spatial learning and memory. During the initial training, the escape latency decreased significantly with increasing training days, as shown in Fig. 3(b), and the repeated-measures ANOVA showed significant main factor of the days in each group (all P values less than 0.001). The reduced escape latency meant that the mice found the platform more quickly, indicating the effectiveness of multi-day training. Gladly, on the fifth day, the escape latencies of both the TMAS_I and TMAS_II groups were significantly lower than those of the sham group (TMAS_I vs. sham: P=0.030; TMAS_II vs. sham: P=0.029), the swimming distance of the TMAS_II group was significantly lower than that of the sham group (TMAS_II vs. sham: P=0.012), indicating that TMAS enhanced spatial memory capacity. While there was no significant difference in the TUS groups compared to the sham group. ANOVA showed an interaction effect, and post hoc indicated the escape latencies of the TUS_II (P=0.001) was significantly lower than that of the TUS_I group, suggesting that the modulatory effect of TUS is related to ultrasound intensity. During the space probe test, larger number of platform crossings and quadrant occupancy reflected firmer spatial memory. As shown in Fig. 3(c), the number of platform crossings in the TMAS_II group was significantly higher than that in the sham group (P=0.030), and ANOVA showed significant main effect of the stimulation modality (F(1, 28)=4.634, p=0.05). While, no significant difference was shown in the quadrant occupancy.

The reversal MWM procedure was used to assess the flexibility of spatial learning and reconstruction of spatial memory. During the reversal training, the escape latencies of the TUS_II group and the TMAS_II group were shorter than that of the sham group (TUS_II vs. sham: P=0.036; TMAS_II vs. sham: P=0.022), while the swimming distance showed no significant difference. In the reversal probe test, as shown in Fig. 3(e), the number of platform crossings in the TMAS_II group (P=0.014) and the number of quadrant occupancies in the TUS_II group (P=0.048) were significantly higher than those in the sham group. Furthermore, stimulation × intensity ANOVA showed that both stimulation modality and intensity had significant effects, revealing significantly higher platform crossing numbers (F (1,28) =6.542, p=0.018) and quadrant occupancy (F (1, 28) =5.478, p=0.029) in the TMAS groups than in the TUS groups and with stimulation at high ultrasound intensity (F (1,28) =4.719, p=0.040; F (1,28) =4.896, p=0.038, respectively) than at low ultrasound intensity. The flexibility of spatial learning and reconstruction of spatial memory were enhanced after TUS/TMAS stimulation, and ultrasound intensity affected the modulatory effect.

C. TMAS enhanced synaptic plasticity between DG and PP

In the electrophysiological experiment, the population spike (PS) from PP to DG (Fig. 4(a)) were recorded at input-output experiment (I/O), baseline and after theta burst stimulation (TBS). I/O function (Fig.4(b)) showed that TUS/TMAS did not affect basal synaptic transmission at two test ultrasound intensities. The average amplitude of PS between the first and the second peak were calculated to reflect synaptic function. As shown in Fig. 4(c), the PS amplitudes after TBS were larger than that at baseline for a long time, reflected LTP in synaptic plasticity. Specifically, the ratio of PS amplitudes during the last 30 minutes after TBS to baseline was calculated to quantify the degree of LTP. As shown in Fig. 4(d), the degree of LTP for TMAS_I (118.299±3.835%) and TMAS_II (128.812±5.538%) were higher than for other groups (sham:113.621±4.411%; TUS_I:113.552±5.504%; TUS_II:116.613±4.919%;). At 5 W/cm2, TMAS-induced LTP were 113.4% compared to the sham group and 110.5% compared to TUS. When compared to the sham group, only TMAS_II significantly improved the LTP (P=0.032).

D. TMAS significantly enhanced relative power of high gamma oscillation

Power spectral analysis was performed at the theta, low gamma and high gamma bands. The power of each band was normalized by the total power. The representative raw LFP and time-domain signals of each frequency band are shown in Fig. 5(a). For the theta band (Fig. 5(b)), the relative power did not show a significant difference among groups. For both the low gamma band (Fig. 5(c)) and high gamma band (Fig. 5(d)), the relative power in the TMAS group (low gamma band: TMAS_I: 3.390±0.400%, TMAS_II: 3.47±0.617%; high gamma band: TMAS_I: 0.740±0.148%, TMAS_II: 1.060±0.155%) was higher than that in the TUS group (low gamma band:

TUS_I:1.840±0.271%; TUS_II:3.000±0.353%; high gamma band: TUS_I:0.570±0.099%; TUS_II:0.560±0.114%), and stimulation × intensity ANOVA showed significant main effects of stimulation modality (F (1,28) =10.017, P=0.004, for the low gamma band, F (1,28) =6.613, P=0.016, for the high gamma band). Notably, the relative power of the high gamma band in the TMAS_II group was significantly higher than that in the sham group (sham: 0.570±0.088% vs TMAS_ II: 1.060±0.155%, P=0.027), indicating an outstanding improvement by TMAS.

E. TMAS enhanced synchronization of neural oscillations between DG and PP

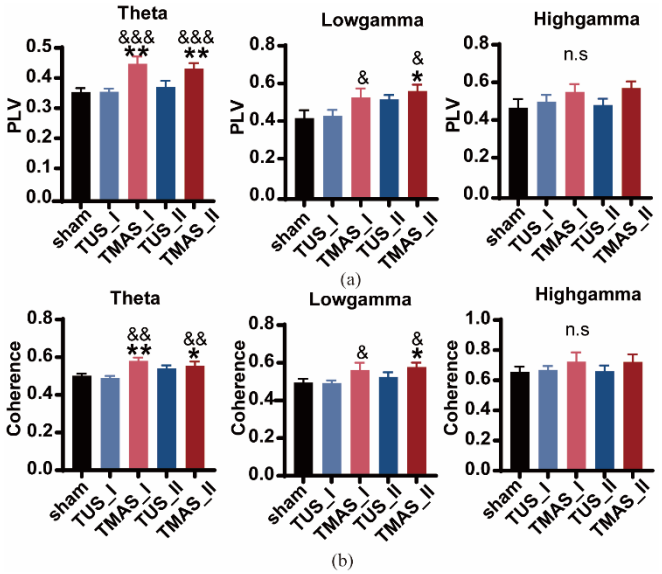

Fig. 6 Effects of TMAS and TUS on synchronization of neural oscillations. (a) The statistical mean results of the PLVs. (b) The statistical mean results of the coherence. *P<0.05, **P<0.01 vs. the Sham group. &P<0.05, &&P<0.01, &&&P<0.001 stimulation modality effect.

Synchronization of neural oscillations between DG and PP was measured using PLV and coherence. PLV measures the synchronization in the signal phase from the DG and PP regions. As shown in Fig. 6(a), compared to those of the sham group, the PLV values of the TMAS_I group were higher in the theta band (sham: 0.353±0.013 vs TMAS_I: 0.447±0.024, P=0.004), and the PLV values of the TMAS_II group were significantly higher in both the theta (sham: 0.353±0.013 vs TMAS_ II: 0.431±0.019, P=0.004) and low gamma bands (sham: 0.416±0.042 vs TMAS_ II: 0.560±0.033, P=0.017). Two-way ANOVA for PLV showed that only stimulus modality had a significant effect on theta (F(1,28)=16.194, P=0.000) and low gamma bands (F(1,28)=4.327, P=0.047), and in these rhythms, the TMAS group had higher phase synchronization and more effective information transfer in DG-PP areas than the TUS group.

Coherence was used to reflect the synchronization in the frequency domain of signals between DG and PP regions. The results (Fig. 6(b)) showed that TMAS_I enhanced the coherence in the theta band (sham: 0.502±0.011 vs TMAS_I: 0.581±0.017, P=0.002), and TMAS_II enhanced the coherence both in the theta band (sham: 0.502±0.011 vs TMAS_ II: 0.555±0.019, P=0.022) and in the low gamma band (sham: 0.495±0.020 vs TMAS_ II: 0.578±0.033, P=0.024), while there was no significant difference between the TUS groups and the sham group. The results of the comparison between the stimulation groups were similar to those for PLV, by which stimulation modality also showed significant effects in the theta (F(1,28)=9.773, P=0.004) and low gamma bands (F(1,28)=5.103, P=0.032), with higher coherence values in the TMAS groups than in the TUS groups.

F. TMAS strengthened theta-gamma coupling in DG

In hippocampus, gamma oscillations reflect local domains of information processing, theta oscillations are dynamically entrained across the network. The cross-frequency phase-amplitude coupling (PAC) provides an effective means to integrate activity across different spatial and temporal scales. The PAC was measured using the modulation index of the phase of the theta rhythms to the amplitude of the gamma rhythms in DG. As shown in Fig. 7(a), the PAC in this study mainly manifested in theta-low gamma (20-40Hz), and theta-high gamma (60-90Hz). The MI values were calculated and compared in Fig. 7(b). The MI value of the TMAS_I group was significantly higher than that of the sham group in both theta-low gamma coupling (P=0.040) and theta-high gamma (P=0.021) coupling, while the MI value of the TMAS_II group was significantly higher in the theta-high gamma coupling (P=0.019). Further stimulation × intensity ANOVA revealed that in the theta-low gamma coupling, the magnitude of the PAC was closely related to stimulation modality (F(1,28)=6.688, P=0.015); meanwhile, in the theta-high gamma band, the MI values of the TMAS groups were higher than those of the TUS groups, although stimulation modality just showed a slightly significant effect (F(1,28)=3.994, P=0.055).

Phase-phase CFC provides a plausible physiological mechanism for linking activity that occurs at significantly different rates. Fig. 7(c) showed the phase changes of theta, low gamma, and high gamma oscillations over a fixed time period (1s). The effects of TUS and TMAS on the cross-frequency phase-phase coupling of the DG regions were assessed by n:m PLV). As shown in Fig. 7(d), TMAS-I and TMAS-II were more efficient in enhancing theta- low gamma phase-phase coupling, with significantly higher PLV at 1:6 (TMAS_I: P=0.011; TMAS_II: P=0.024) and 1:8 (TMAS_I: P=0.007; TMAS_II: P=0.010) than sham treatment. For theta- high gamma phase-phase coupling, TMAS_I was more efficient at 1:10 (P=0.044), 1:11 (P=0.039) and 1:12 (P=0.029) than sham treatment, while TMAS_II was more efficient at 1:15 (P=0.006). The cross-frequency phase-phase coupling of the TUS groups were not significantly different from those of the sham group.

G. Synaptic-related and GABAergic protein changed after TUS/TMAS stimulation

To investigate the potential molecular mechanisms of TUS and TMAS on synaptic plasticity and neural activity in mice, the protein levels of the presynaptic membrane marker SYP, postsynaptic marker PSD-95, excitatory receptors NR2A and NR2B, and inhibitory receptor GABAAR were examined. Fig. 8(a) showed the grayscale values of the protein band by

Western blot. As shown in Fig. 8(b), The level of SYP in the TMAS_I and TMAS_II groups were significantly greater than that in the sham group (TMAS_I: P=0.005; TMAS_II: P<0.001), while SYP levels were significantly reduced in the TUS_I group relative to those in the sham group (P=0.002). For the postsynaptic marker PSD-95 (Fig. 8(c)), TMAS_I and TMAS_II showed significantly increased levels (TMAS_I: P=0.033; TMAS_II: P=0.003). Comparing the results of each stimulation group, stimulation modality had a significant effect for both SYP and PSD95, with higher protein levels in the TMAS group than in the TUS group. In addition, stimulation modality had an interaction effect with intensity, and post hoc analysis showed that for TUS, synapse-related protein levels were significantly higher in TUS with high ultrasound intensity than in TUS with low ultrasound intensity.

For excitatory (Fig. 8(d-e)) and inhibitory (Fig. 8(f)) receptor-related proteins, TMAS_I, TMAS_II and TUS_II all showed greater levels of NR2A (TMAS_I: P=0.007; TMAS_II: P<0.001; TUS_II: P=0.091), NR2B (TMAS_I: P<0.001; TMAS_II: P<0.001; TUS_II: P=0.003) and GABAAR (TMAS_I: P=0.009; TMAS_II: P=0.002; TUS_II: P=0.013). The TUS_I group showed significant reductions in NR2A (P=0.016), NR2B (P=0.04) and GABAAR levels (P=0.019). Furthermore, two-way ANOVA showed that for excitatory receptor proteins and inhibitory receptor proteins, the level was significantly higher in the TMAS group than in the TUS group, and the protein level in TUS with high ultrasound intensity was higher than that with low ultrasound intensity.

IV. Discussion

In this study, TMAS was used and compared with TUS, in the expectation that the combined action of ultrasound and coupled electric fields would achieve better modulatory effects. We found that both TMAS and TUS enhanced memory, with TMAS being more effective. Specially, our results showed TMAS markedly modulate hippocampus long-term synaptic plasticity and rhythmic oscillations in C57 mice.

TMAS enhanced synaptic plasticity and cognitive behaviors

To suggest TUS and TMAS as treatment modalities, it is of utmost importance to ascertain their safety. In 90% of the existing studies, ultrasound intensities of 0.2-6 W/cm^2 were used targeting small animal's brain, which were proven to be effective and safe. We used ultrasound intensities at 3W/cm2 and 5W/cm^2, falling within the safe range, and the open-field results showed that prolonged stimulation did not cause anxiety in mice. Several studies have demonstrated that ultrasound stimulation enhances learning and cognitive abilities in animals [27, 22]. For TMAS, Wang's study [20] showed significant improvement in water maze behavior in PD mice. However, the specific action and differences between TUS and TMAS in improving cognition on C57 mice were still unclear. Therefore, two kinds of behavioral tasks were carried out to evaluate modulatory effect on memory. We found that both TUS and TMAS enhanced short-term memory (Fig. 2), with no difference in the modulatory effects. As for spatial learning and memory (Fig. 3(C)), only TMAS showed significant enhancement. We speculated that the superiority of TMAS in enhancing spatial learning and memory may be related to the modulation of long-term synaptic plasticity and rhythmic oscillations by complex effects in TMAS.

Further, the modulatory effects of TUS and TMAS were compared at the synaptic level. LTP is a cytological mechanism of learning memory and is closely related to calcium ions. Niu [11] found that TUS stimulation for 5 minutes induced sustained LTD but not LTP, possibly due to the limited concentration of calcium ions aggregated by TUS. Niu [11] found that TUS stimulation for 5 minutes induced sustained LTD but not LTP, possibly due to the limited concentration of calcium ions aggregated by TUS. Huang [9] found that prolonged TUS increased the frequency of excitatory spontaneous postsynaptic currents (EPSC) in CA1 hippocampal pyramidal neurons and concluded that this was evidence that TUS induced sustained synaptic plasticity. Further, in Huang's study, TUS did not increase the EPSC amplitude of CA1 hippocampal pyramidal neurons. Both studies showed that TUS can modulate synaptic plasticity, but is ineffective in modulating electrophysiological properties associated with synaptic plasticity. The results of the present study showed that TUS stimulation for 7 days failed to elevate LTP when compared to the sham group (Fig. 4), which indicated suboptimal efficiency in modulating synaptic plasticity. Whereas, after adding the coupling electric field, the LTP of TMAS group significantly increased compared to sham group, reflecting enhanced synaptic plasticity. The question that then arose was what mediated the differences in LTP modulation by TUS and TMAS. So, we evaluated the levels of synaptic plasticity-associated proteins. In LTP, calcium inward flow through NMDA receptors (NR2A and NR2B) plays a central role in recruitment-specific intracellular signaling cascades [28]. Previously, NMDA receptors in cultured neurons were found to be mechanosensitive [29]. Wang [30] found that TUS increased the levels of NR2B in vascular dementia rats. Our results (Fig. 8) also showed the elevation on NR2B by TUS. Compared to TUS, we found that TMAS not only elevated the expression levels of NR2B to a greater extent, but also significantly enhanced NR2A SYP, and PSD-95. SYP is a specific presynaptic vesicle membrane protein that reflects the efficacy of synaptic transmission and plays a major role in Ca-dependent neurotransmitter release [31]; PSD-95 is involved in glutamatergic transmission and is intimately involved with LTP induction and eventual maintenance [32]. Wang's [20]and Zhou's [33] studies showed that TMAS increased LTP in PD rats mainly dependent on PSD95. We found that both SYP and PSD95 play important roles in enhancing synaptic plasticity in TMAS. The difference in the degree of regulation on NMDA receptors and the ability to modulate PSD95 and SYP led to differences in the modulation of LTP by TUS and TMAS. The superior modulation on synaptic plasticity by TMAS over TUS may be attributed to the complex action of its multi-physics fields.

TMAS enhanced hippocampal oscillations

Then, the modulatory effects of TUS and TMAS on rhythmic oscillations were investigated. Theta rhythms are associated with the formation and retrieval of short-term and spatial memories [34], and gamma rhythms are associated with attention and retention of memory-related information [35]. Previous studies have shown that the effect of TUS was highly

dependent on the ultrasound intensity [12, 13, 36]. Our results showed that increasing the ultrasound intensity from 3W/cm^2 (ultrasound pressure: 0.21 Mpa) to 5W/cm^2 (ultrasound pressure: 0.27 Mpa) resulted in an enhancement of TUS modulatory effect in terms of behavioral tests, LTP, and protein expression. But in rhythmic oscillations, TUS did not have a significant effect on the power in either the theta or gamma bands, even increasing ultrasound intensity from 3W/cm^2 to 5W/cm^2 (Fig. 5), reflected suboptimal efficiency in modulating rhythmic oscillations. We speculated that this might be due to the higher ultrasound intensity required for TUS-modulated rhythmic oscillations. In Xie's [12] study on C57 mice, TUS enhanced the power of rhythmic oscillations only when the ultrasonic pressure exceeded 0.6MPa. In contrast, the relative power of gamma oscillations in the TMAS group was significantly greater than not only that in sham group, but also that in the TUS group at the same ultrasound parameters, which may be due to the additional coupled electric field.

Cognition occurs through the coordinated activity of neural networks operating at different spatial and temporal scales. Synchronization can contribute to synaptic plasticity by correlating the timing of presynaptic and postsynaptic potentials [37, 38]. Theta oscillations synchronization can effectively read-out information held in working memory, thus facilitating it [39]. The synchronization of gamma oscillations underlies the replay of previously stored memories, thus supporting memory extraction and consolidation [40]. In this study, PLV and coherence measured phase and power synchronization between DG and PP brain regions. Results indicated TMAS enhanced synchronization in theta and gamma bands within the hippocampal network, possibly improving working memory read-out and replay, thus influencing behaviors in NOR and the MWM. TUS, using similar ultrasonic parameters, did not significantly enhance neural oscillation synchronization.

Cross-frequency coupling generally manifests as the coupling phenomenon between low-frequency rhythms and high-frequency rhythms in a nucleus mass. CFC is strongly correlated with spatial working memory, especially for the theta-high gamma PAC [41]. Weakened PAC strength is strongly associated with multiple cognitive dysfunctions [42, 43], and cross-frequency phase coupling can support multiple time-scale control of neuronal spikes [44]. A previous study found that prolonged TUS stimulation could restore PAC intensity in AD model mice [10]. Yuan Yi [13] used TUS at different spatial-average, pulse-average acoustic intensities to stimulate the hippocampus of normal rats and found that TUS at 3.9 W/cm^2 had no effect on PAC intensity, while TUS above 9.6 W/cm^2 enhanced PAC. In this study, TUS at low acoustic intensities (3 W/cm^2 and 5 W/cm^2) did not tend to enhance PAC intensity, which is consistent with the results of Yuan Yi's study. These studies all demonstrated that TUS modulation of PAC may require higher ultrasound intensity. With the same ultrasonic parameters as TUS, our findings indicate that TMAS notably increased theta-gamma phase-amplitude coupling (Fig. 7). This enhancement in theta-gamma PAC correlates with improved spatial working memory, as observed in the MWM.

How TMAS enhanced the modulatory effect of TUS?

Taking all together, we found that TMAS enhanced the modulatory effect on hippocampal rhythmic oscillations and synapses. Increasingly, it has been found that TUS mainly acts through mechanical forces to activate specific mechanosensitive ion channels, such as TRPA1 [14] and peizo1 [15], allowing calcium ion inward flow. While, the most common spontaneously active ion channels found in hippocampus neurons were large-conductance cation channels, which demonstrated clear voltage-dependence on electrical stimulation [45]. Thus, the combined effect of mechanical forces and electric fields in TMAS may elicit a broader response. Moreover, in contrast to TUS, which may require the application of multiple pulses to alter the membrane potential, each electrical pulse applied by electrical field on the presynaptic axon results in a correlated increase in voltage [11]. These may account for the superiority of TMAS.

As for the hippocampal oscillations, the enhancement on gamma oscillation as well as its associated synchronization and cross-frequency coupling by TMAS was outstanding. But why gamma oscillations? Gamma oscillations are thought to primarily characterize the activity of GABAergic interneurons [46, 47]. Rapidly firing parvalbumin (PV) cells are the main GABAergic interneurons in the hippocampus and generate gamma oscillations through inhibition of excitatory pyramidal cells, and the Nav1.1 ion channel is highly expressed in PV cells. In 2012, Verrett et al. [48] enhanced the gamma rhythm by increasing the expression of Nav1.1 in PV cells. The Nav1.1 ion channel is a voltage-gated sodium channel that, to date, has not been shown to be mechanosensitive. Therefore, we speculate that the coupled electric field in TMAS may act on PV interneurons by activating the Nav1.1 ion channel, which in turn enhances the gamma rhythm. GABAA receptors are important inhibitory receptors in the mature brain, and impairment of GABAA receptors results in excitatory neuronal hyperexcitability leading to cognitive impairment, which is the causal mechanism of many neurological disorders [49-51]. In the present study, the expression level of GABAAR receptors was elevated by TMAS, and the performance of TMAS was significantly superior to that of TUS. The enhanced gamma oscillation and elevated expression of GABAAR receptors both promote the brain's adaptive response to excitatory drives [52], crucial for flexible adaptation to novel events.

Future works

The paper aims to explore TMAS and TUS effects on the hippocampal region, currently using a static magnetic field, which is more realizable. Recent research on static magnetic fields reveals conflicting findings on their effects on cortical excitability. One possible explanation for the shift from short-term to long-term static magnetic field stimulation effects is that short-term exposure (10 min) may reduce glutamatergic excitation, while longer exposure (30 min) may decrease glutamatergic excitation and phasic GABAergic inhibition [53]. Our study, with brief exposure (5 min/day for 7 days), didn't focus solely on static magnetic field effects on TMAS. In the event of improperly selected parameters, the static magnetic field may engender an inhibitory response counterproductive to the intended outcome. Future work will delve into optimizing these parameters in TMAS.

Future considerations also include TMAS with alternating magnetic fields. The combined use of alternating magnetic fields such as TMS can provide a more precise magnetic field and a stronger electric field for TMAS. On the other hand, TMS

brings about a non-negligible stimulation effect in the cortex, so TMAS with alternating magnetic fields requires careful consideration of target and non-target areas in the future work.

V. Conclusion

The present study demonstrated the beneficial effects of TMAS under the ultrasound parameters used in this paper on improving cognition behaviors, synaptic plasticity, and related protein levels, with a performance superior to that of TUS. TMAS significantly facilitated gamma oscillation power, synchronization of the theta and gamma bands, and theta-gamma phase-phase coupling and phase-amplitude coupling, while TUS did not tend to enhance at present acoustic parameters. The superior performance of TMAS over TUS under the ultrasound parameters used in this paper may be attributed to the complex action of its multi-physics fields. This study revealed the great potential of TMAS for applications in neurological diseases.

References

[1] L. Buntwal, M. Sassi, A. H. Morgan, Z. B. Andrews, and J. S. Davies, "Ghrelin-Mediated Hippocampal Neurogenesis: Implications for Health and Disease," *Trends Endocrinol Metab*, vol. 30, pp. 844-859, Nov. 2019.

[2] T. Toda, S. L. Parylak, S. B. Linker, and F. H. Gage, "The role of adult hippocampal neurogenesis in brain health and disease," *Mol Psychiatry*, vol. 24, pp. 67-87, Jan. 2019.

[3] C. Wang *et al.*, "Tactile modulation of memory and anxiety requires dentate granule cells along the dorsoventral axis," *Nat Commun*, vol. 11, p. 6045, Nov. 2020.

[4] X. Zhang *et al.*, "Hippocampal network oscillations in APP/APLP2-deficient mice," *PLoS One*, vol. 8, p. e61198, Jan. 2013.

[5] K. B. J. Franklin, K. B. J. Franklin and G. Paxinos, *The mouse brain in stereotaxic coordinates*, 2nd ed. ed. San Diego: Academic Press, 2001.

[6] S. Kim *et al.*, "Transcranial focused ultrasound stimulation with high spatial resolution," *Brain Stimul*, vol. 14, pp. 290-300, Mar. 2021.

[7] H. B. Kim *et al.*, "Prolonged stimulation with low-intensity ultrasound induces delayed increases in spontaneous hippocampal culture spiking activity`," *J Neurosci Res*, vol. 95, pp. 885-896, Mar. 2017.

[8] W. J. Tyler *et al.*, "Remote excitation of neuronal circuits using low-intensity, low-frequency ultrasound," *PLoS One*, vol. 3, p. e3511, Jan. 2008.

[9] X. Huang *et al.*, "Transcranial Low-Intensity Pulsed Ultrasound Modulates Structural and Functional Synaptic Plasticity in Rat Hippocampus," *IEEE Trans Ultrason Ferroelectr Freq Control*, vol. 66, pp. 930-938, May. 2019.

[10] M. Park *et al.*, "Effects of transcranial ultrasound stimulation pulsed at 40 Hz on Aβ plaques and brain rhythms in 5×FAD mice," *Translational Neurodegeneration*, vol. 10, p. 48, 2021.

[11] X. Niu, K. Yu and B. He, "Transcranial focused ultrasound induces sustained synaptic plasticity in rat hippocampus," *Brain Stimul*, vol. 15, pp. 352-359, Mar. 2022.

[12] Z. Xie, J. Yan, S. Dong, H. Ji, and Y. Yuan, "Phase-locked closed-loop ultrasound stimulation modulates theta and gamma rhythms in the mouse hippocampus," *Front Neurosci*, vol. 16, p. 994570, Jan. 2022.

[13] Y. Yuan, J. Yan, Z. Ma, and X. Li, "Noninvasive Focused Ultrasound Stimulation Can Modulate Phase-Amplitude Coupling between Neuronal Oscillations in the Rat Hippocampus," *Front Neurosci*, vol. 10, p. 348, Jan. 2016.

[14] S. J. Oh *et al.*, "Ultrasonic Neuromodulation via Astrocytic TRPA1," *Curr Biol*, vol. 29, pp. 3386-3401.e8, Oct. 2019.

[15] S. Yoo, D. R. Mittelstein, R. C. Hurt, J. Lacroix, and M. G. Shapiro, "Focused ultrasound excites cortical neurons via mechanosensitive calcium accumulation and ion channel amplification," *Nature Communications*, vol. 13, Jan. 2022.

[16] S. J. Norton, "Can ultrasound be used to stimulate nerve tissue?" *Biomed Eng Online*, vol. 2, p. 6, Mar. 2003.

[17] H.Li. *et al.*, " A preliminary investigation of a focused electrical stimulation method based on the magnetoacoustic coupling effect" *Journal of Biomedical Engineering Research*, vol. 34, pp. 201-206, Dec. 2015.

[18] Y. Yuan, Y. Chen and X. Li, "Theoretical Analysis of Transcranial Magneto-Acoustical Stimulation with Hodgkin-Huxley Neuron Model," *Front Comput Neurosci*, vol. 10, p. 35, Jan. 2016.

[19] S. Zhang *et al.*, "Effect of Transcranial Ultrasonic–Magnetic Stimulation on Two Types of Neural Firing Behaviors in Modified Izhikevich Model," *IEEE Transactions on Magnetics*, vol. 54, Mar. 2018.

[20] Y. Wang *et al.*, "Transcranial Magneto-Acoustic Stimulation Improves Neuroplasticity in Hippocampus of Parkinson's Disease Model Mice," *Neurotherapeutics*, vol. 16, pp. 1210-1224, Oct. 2019.

[21] H. Wang *et al.*, "Comparative Study of Transcranial Magneto-Acoustic Stimulation and Transcranial Ultrasound Stimulation of Motor Cortex," *Frontiers in Behavioral Neuroscience*, vol. 13, p. 241, Oct. 2019.

[22] W. T. Lin, R. C. Chen, W. W. Lu, S. H. Liu, and F. Y. Yang, "Protective effects of low-intensity pulsed ultrasound on aluminum-induced cerebral damage in Alzheimer's disease rat model," *Sci Rep*, vol. 15, p. 9671, Apr. 2015.

[23] F. Mormann *et al.*, "Phase/amplitude reset and theta-gamma interaction in the human medial temporal lobe during a continuous word recognition memory task," *Hippocampus*, vol. 15, pp. 890-900, Jan. 2005.

[24] C. Zheng, K. W. Bieri, Y. T. Hsiao, and L. L. Colgin, "Spatial Sequence Coding Differs during Slow and Fast Gamma Rhythms in the Hippocampus," *Neuron*, vol. 89, pp. 398-408, Jan. 2016.

[25] S. Aydin, "Comparison of power spectrum predictors in computing coherence functions for intracortical EEG signals," *Ann Biomed Eng*, vol. 37, pp. 192-200, Jan. 2009.

[26] F. Chu *et al.*, "Transcranial Magneto-Acoustic Stimulation Attenuates Synaptic Plasticity Impairment through the Activation of Piezo1 in Alzheimer's Disease Mouse Model," *Research (Wash D C)*, vol. 6, p. 0130, Jan. 2023.

[27] K. Eguchi *et al.*, "Whole-brain low-intensity pulsed ultrasound therapy markedly improves cognitive dysfunctions in mouse models of dementia - Crucial roles of endothelial nitric oxide synthase," *Brain Stimul*, vol. 11, pp. 959-973, Sep. 2018.

[28] J. P. Dupuis, O. Nicole and L. Groc, "NMDA receptor functions in health and disease: Old actor, new dimensions," *Neuron*, May. 2023.

[29] P. Paoletti and P. Ascher, "Mechanosensitivity of NMDA receptors in cultured mouse central neurons," *Neuron*, vol. 13, pp. 645-55, Sep. 1994.

[30] F. Wang *et al.*, "Low-Intensity Focused Ultrasound Stimulation Ameliorates Working Memory Dysfunctions in Vascular Dementia Rats via Improving Neuronal Environment," *Front Aging Neurosci*, vol. 14, p. 814560, Jan. 2022.

[31] U. Schmitt, N. Tanimoto, M. Seeliger, F. Schaeffel, and R. E. Leube, "Detection of behavioral alterations and learning deficits in mice lacking synaptophysin," *Neuroscience*, vol. 162, pp. 234-43, Aug. 2009.

[32] J. C. Beique and R. Andrade, "PSD-95 regulates synaptic transmission and plasticity in rat cerebral cortex," *J Physiol*, vol. 546, pp. 859-67, Feb. 2003.

[33] X. Zhou *et al.*, "High-Resolution Transcranial Electrical Simulation for Living Mice Based on Magneto-Acoustic Effect.," *Frontiers in neuroscience*, vol. 13, p. 1342, Jan. 2019.

[34] N. A. Herweg, E. A. Solomon and M. J. Kahana, "Theta Oscillations in Human Memory," *Trends Cogn Sci*, vol. 24, pp. 208-227, Mar. 2020.

[35] M. Lundqvist *et al.*, "Gamma and Beta Bursts Underlie Working Memory," *Neuron*, vol. 90, pp. 152-164, Apr. 2016.

[36] Y. Yuan *et al.*, "The Effect of Low-Intensity Transcranial Ultrasound Stimulation on Neural Oscillation and Hemodynamics in the Mouse Visual Cortex Depends on Anesthesia Level and Ultrasound Intensity," *IEEE Trans Biomed Eng*, vol. 68, pp. 1619-1626, May. 2021.

[37] J. Fell and N. Axmacher, "The role of phase synchronization in memory processes," *Nat Rev Neurosci*, vol. 12, pp. 105-18, Feb. 2011.

[38] M. J. Jutras and E. A. Buffalo, "Synchronous neural activity and memory formation," *Curr Opin Neurobiol*, vol. 20, pp. 150-5, Apr. 2010.

[39] S. N. Jacob, D. Hahnke and A. Nieder, "Structuring of Abstract Working Memory Content by Fronto-parietal Synchrony in Primate Cortex," *Neuron*, vol. 99, pp. 588-597.e5, Aug. 2018.

[40] M. F. Carr, M. P. Karlsson and L. M. Frank, "Transient slow gamma synchrony underlies hippocampal memory replay," *Neuron*, vol. 75, pp. 700-13, Aug. 2012.

[41] I. Alekseichuk, Z. Turi, D. L. G. Amador, A. Antal, and W. Paulus, "Spatial Working Memory in Humans Depends on Theta and High

Gamma Synchronization in the Prefrontal Cortex," *Curr Biol*, vol. 26, pp. 1513-1521, Jun. 2016.
[42] R. T. Canolty and R. T. Knight, "The functional role of cross-frequency coupling," *Trends Cogn Sci*, vol. 14, pp. 506-15, Nov. 2010.
[43] A. Hyafil, A. L. Giraud, L. Fontolan, and B. Gutkin, "Neural Cross-Frequency Coupling: Connecting Architectures, Mechanisms, and Functions," *Trends Neurosci*, vol. 38, pp. 725-740, Nov. 2015.
[44] M. A. Belluscio, K. Mizuseki, R. Schmidt, R. Kempter, and G. Buzsaki, "Cross-frequency phase-phase coupling between theta and gamma oscillations in the hippocampus," *J Neurosci*, vol. 32, pp. 423-35, Jan. 2012.
[45] O. A. Fedorenko and S. M. Marchenko, "Ion channels of the nuclear membrane of hippocampal neurons," *Hippocampus*, vol. 24, pp. 869-76, Jul. 2014.
[46] J. A. Cardin *et al.*, "Driving fast-spiking cells induces gamma rhythm and controls sensory responses," *Nature*, vol. 459, pp. 663-7, Jun. 2009.
[47] V. S. Sohal, F. Zhang, O. Yizhar, and K. Deisseroth, "Parvalbumin neurons and gamma rhythms enhance cortical circuit performance," *Nature*, vol. 459, pp. 698-702, Jun. 2009.
[48] L. Verret *et al.*, "Inhibitory interneuron deficit links altered network activity and cognitive dysfunction in Alzheimer model," *Cell*, vol. 149, pp. 708-21, Apr. 2012.
[49] D. Bi, L. Wen, Z. Wu, and Y. Shen, "GABAergic dysfunction in excitatory and inhibitory (E/I) imbalance drives the pathogenesis of Alzheimer's disease," *Alzheimers Dement*, vol. 16, pp. 1312-1329, Sep. 2020.
[50] T. Enomoto, M. T. Tse and S. B. Floresco, "Reducing prefrontal gamma-aminobutyric acid activity induces cognitive, behavioral, and dopaminergic abnormalities that resemble schizophrenia," *Biol Psychiatry*, vol. 69, pp. 432-41, Mar. 2011.
[51] H. T. Chao *et al.*, "Dysfunction in GABA signalling mediates autism-like stereotypies and Rett syndrome phenotypes," *Nature*, vol. 468, pp. 263-9, Nov. 2010.
[52] S. El-Boustani and M. Sur, "Response-dependent dynamics of cell-specific inhibition in cortical networks in vivo," *Nat Commun*, vol. 5, p. 5689, Dec. 2014.
[53] T. Wang et al., "Exposure to static magnetic field facilitates selective attention and neuroplasticity in rats," *Brain Res Bull*, vol. 189, pp. 111-120, Oct. 2022.

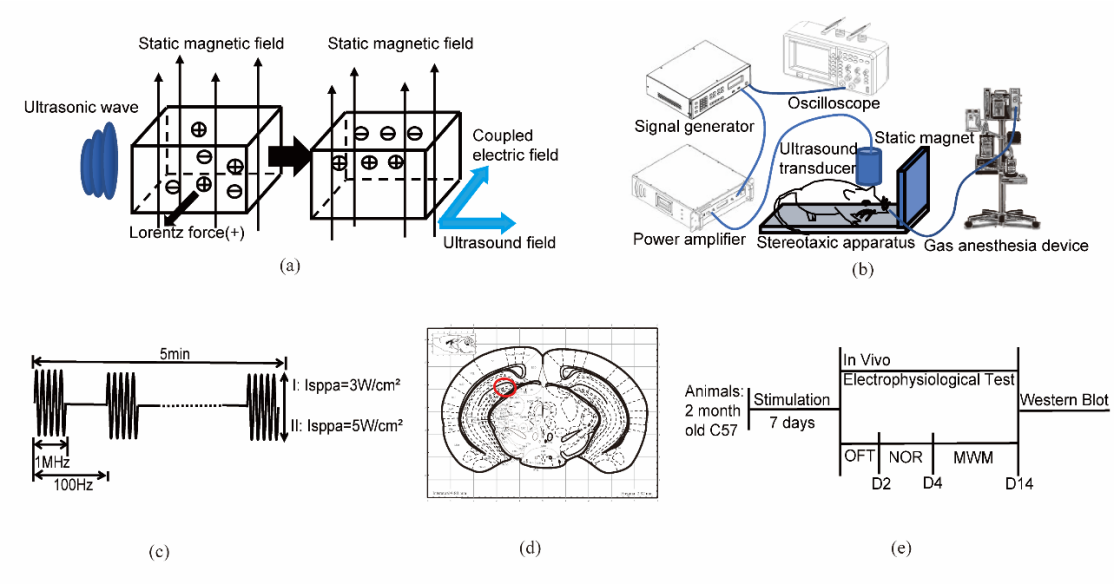

Fig. 1 TMAS and TUS stimulation systems and procedure. (a) Principle of TMAS. (b)Schematic diagram of the TUS/TMAS system for small animals (TUS: without the static magnet, TMAS: with the static magnet. (c) Stimulation signal for TUS/TMAS at different ultrasound intensity. (d) Stimulation target. (e) Experimental Procedure.

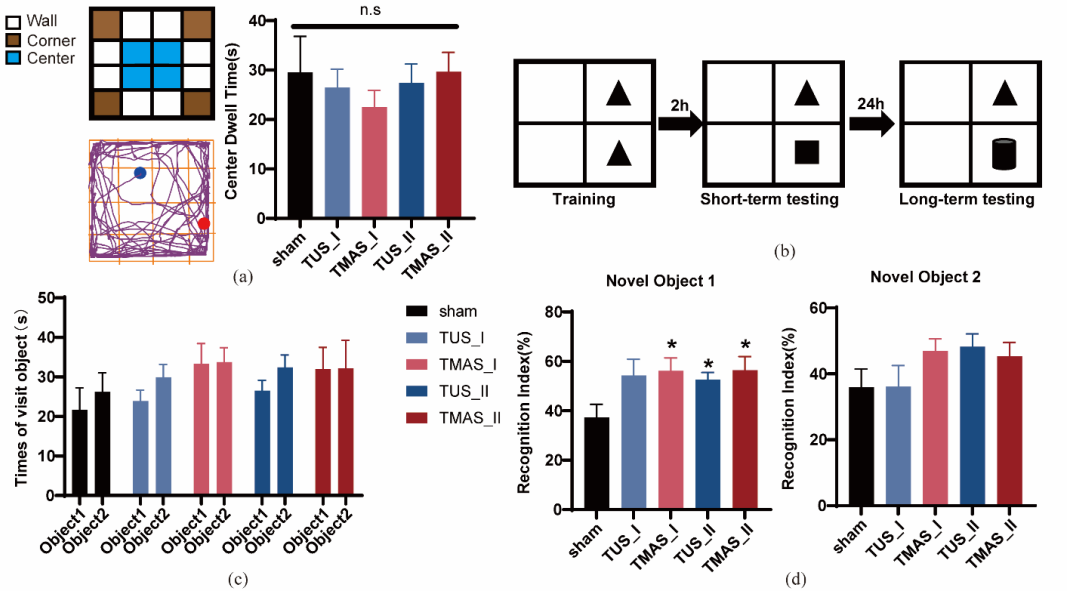

Fig. 2 Open field test and novel object recognition test. (a) Left top, protocol of the open field test. Left bottom, An example of an exploration trace. Right, center dwell time in the open field test. (b) Protocol of the novel object recognition test. (c) Times of object visits in the training session. (d) Left, recognition index in the short-term testing session. Right, recognition index in the long-term testing session. *P<0.05 vs. the sham group.

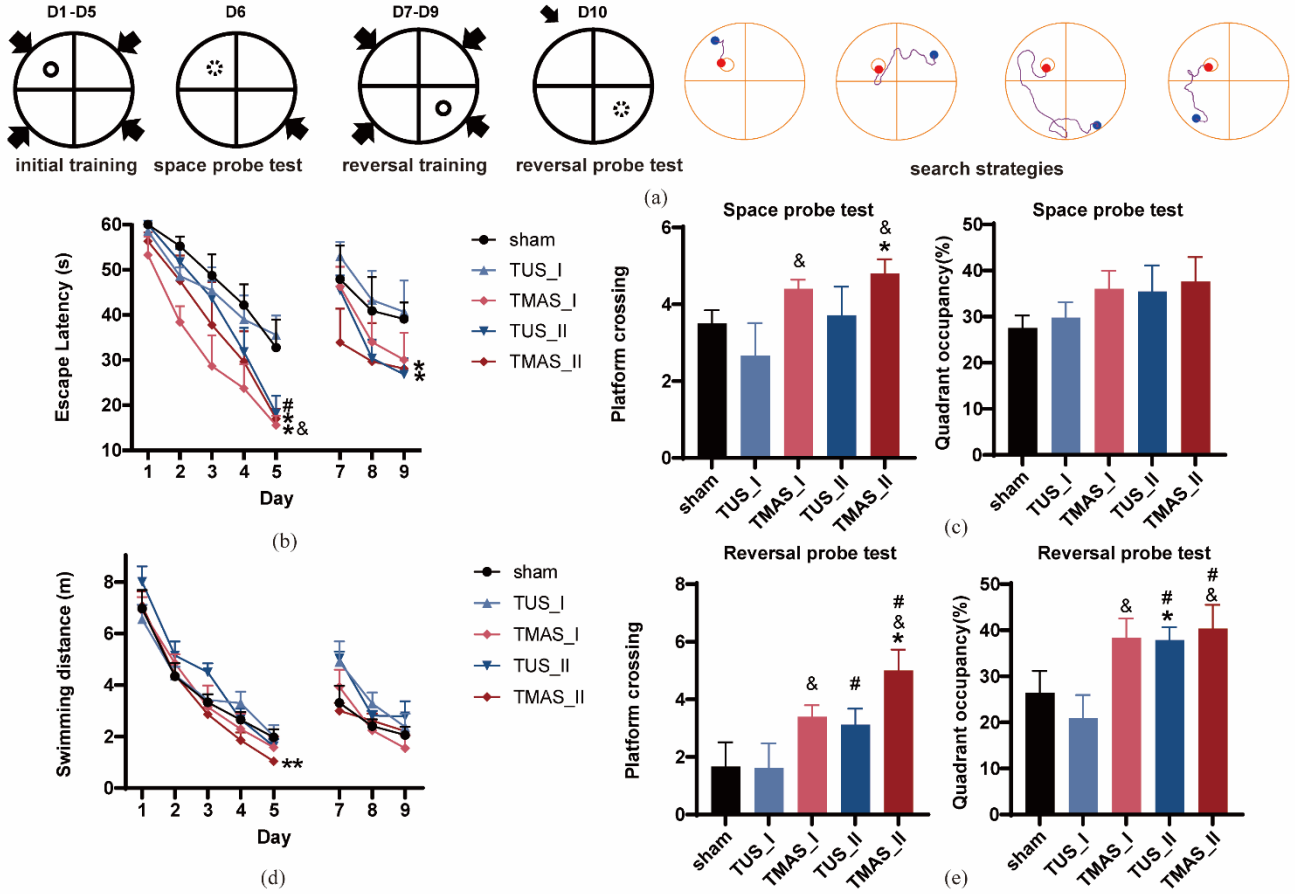

Fig. 3 Morris water maze test. (a) Top, protocol of the Morris water maze test. Bottom, illustration of the search strategies from different quadrants. (b) Escape latencies in the initial training and reversal training. (c) Left, number of platform crossings in the space probe test. Right, percentage of time spent in the corresponding quadrant in the space probe test. (d) Swimming distance during the initial training and reversal training. (e) Left, number of platform crossings in the reversal probe test. Right, percentage of time spent in the corresponding quadrant in the reversal probe test. *P<0.05 vs. the sham group. #P<0.05 intensity effect. &P<0.05 stimulation modality effect

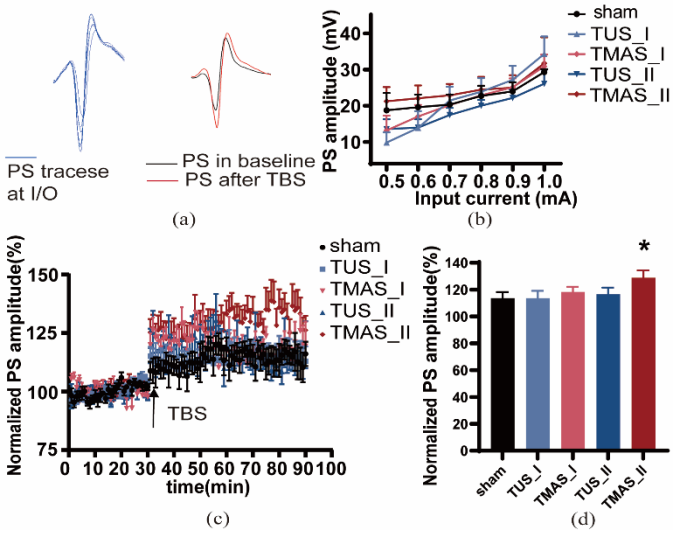

Fig. 4 Normalized slopes of PS in the DG of the mouse hippocampus. (a) Left, sample overlaid traces from single I-O experiments Right, Representative PS curve before and after TBS. (b) I/O function (c) Normalized slopes of PS. (d) Averages of normalized PS during the last 15 min in LTP. **P<0.01 vs. the sham group. &&P<0. 01 stimulation modality effect.

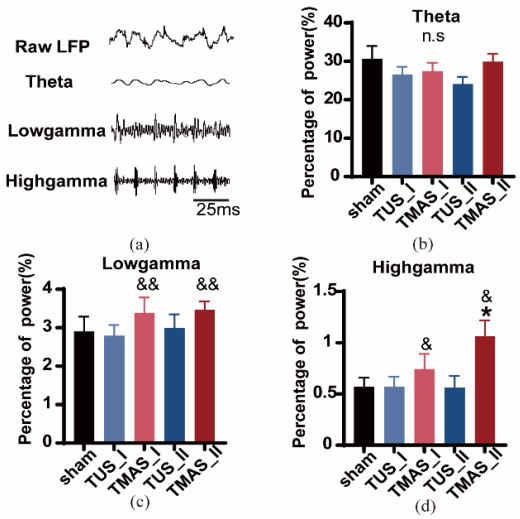

Fig. 5 Effects of TMAS and TUS on the power spectrum. (a) Representative raw trace (1000 ms) of LFP and time-domain signals of each frequency band recorded from DG regions of mice. (b) Averages of normalized power in the theta oscillation. (c) Averages of normalized power in the low gamma oscillation. (d) Averages of normalized power in the high gamma oscillation. *P<0.05 vs. the sham group. &P<0.05, &&P<0.01 stimulation modality effect.

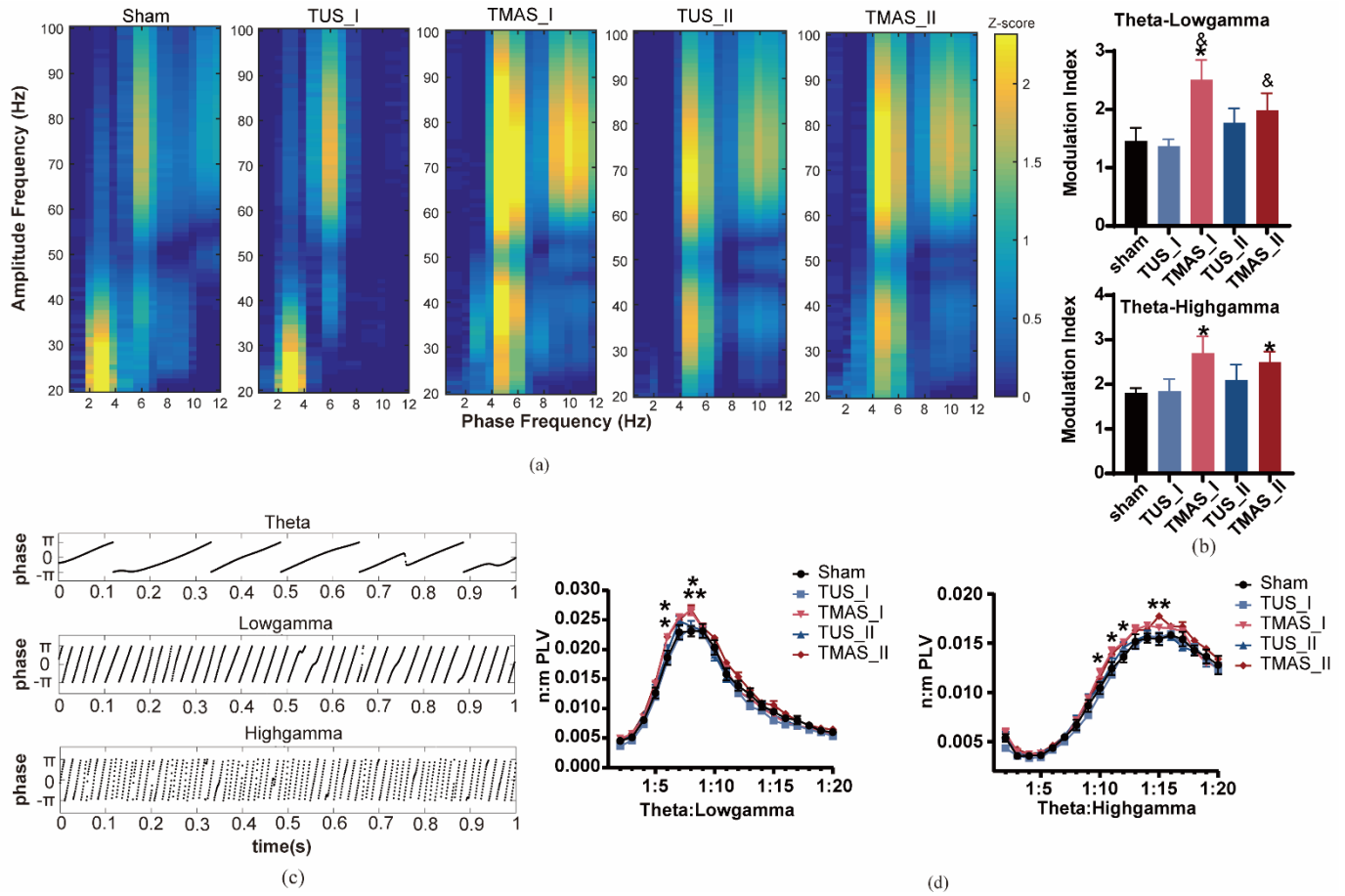

Fig. 7 Effects of TMAS and TUS on cross-frequency coupling. (a) Examples of theta-gamma phase-amplitude coupling in the DG region. (b) Quantification of the PAC modulation index. (c) An example of theta-gamma phase–phase coupling in a sham mouse. (d) The statistical results of theta-low gamma and theta-high gamma PPC in the DG. *P<0.05, **P<0.01 vs. the sham group.

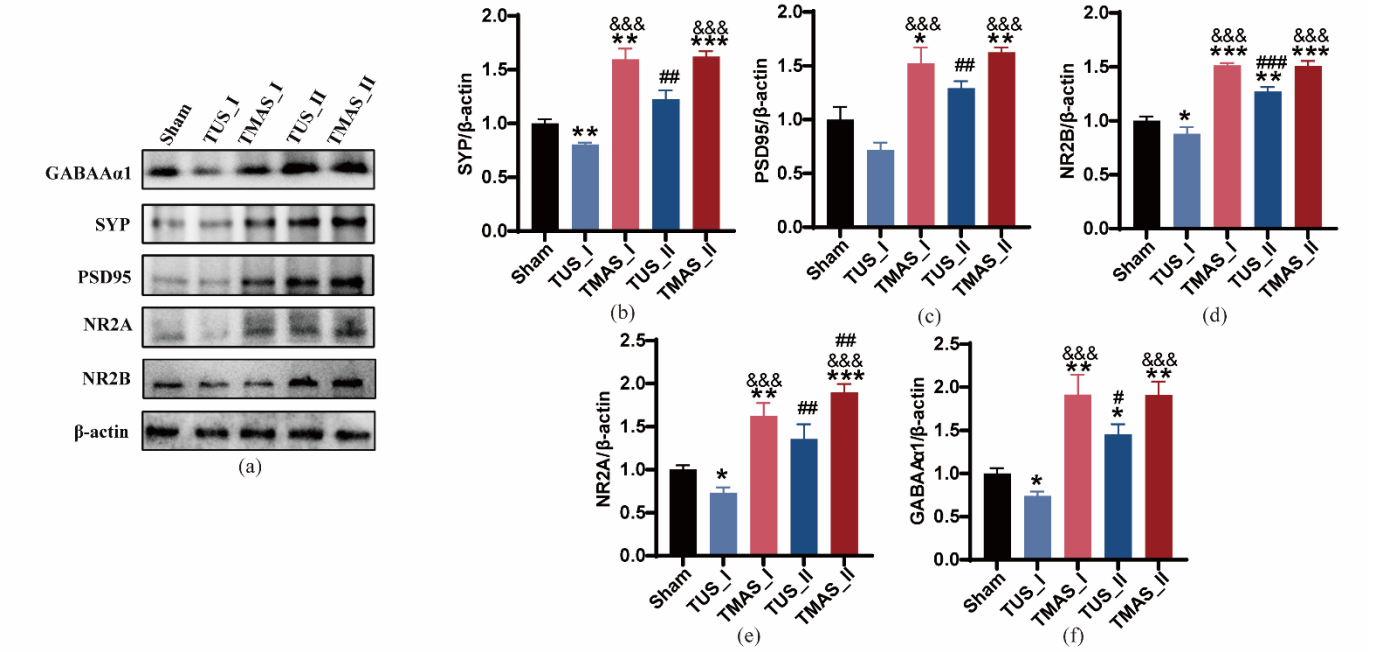

Fig. 8 Effects of TMAS and TUS on protein level. (a) Examples of protein bands in each group. (b) Levels of SYP. (c) Levels of PSD95. (d) Levels of NR2B. (e) Levels of NR2A. (f) Levels of GABAAα1. *P<0.05, **P<0.01, ***P<0.001 vs. the Sham group. #P<0.05, ##P<0.01, ###P<0.001 intensity effect. &&&P<0.001 stimulation modality effect.